Journal of Statistical Physics, Vol. 64, Nos. 3/4, 1991

Cellular Automata Model for the Diffusion Equation

B. Chopard[1] and M. Droz[2]

Received September 19, 1990

We consider a new cellular automata rule for a synchronous random walk on a two-dimensional square lattice, subject to an exclusion principle. It is found that the macroscopic behavior of our model obeys the telegraphists's equation with an adjustable diffusion constant. By construction, the dynamics of our model is exactly described by a linear discrete Boltzmann equation which is solved analytically for some boundary conditions. Consequently, the connection between the microscopic and the macroscopic descriptions is obtained exactly and the continuous limit studied rigorously. The typical system size for which a true diffusive behavior is observed may be deduced as a function of the parameters entering into the rule. It is shown that a suitable choice of these parameters allows us to consider quite small systems. In particular, our cellular automata model can simulate the Laplace equation to a precision of the order $(\lambda/L)^6$, where L is the size of the system and λ the lattice spacing. Implementation of this algorithm on special-purpose machines leads to the fastest way to simulate diffusion on a lattice.

KEY WORDS: Cellular automata; lattice gas; diffusion equation; Telegraphist's equation.

1. INTRODUCTION

Diffusive phenomena play an important role in many areas of physics, chemistry, and biology and constitute an active field of research.

Recently, cellular automata (CA) have proved to be an efficient tool to study systems of many interacting particles. In addition to their well-known applications to fluid mechanics (see, e.g., ref. 1), they have been

[1] Laboratory for Computer Sciences, MIT, Cambridge, Massachusetts 02319.
[2] Département de Physique Théorique, Université de Genève, CH-1211 Geneva 4, Switzerland.

0022-4715/91/0800-0859$06.50/0

used to study diffusion fronts[2] and simple models of chemical reactions[3] and reaction-diffusion processes.[4] Also, the CA approach has been applied to the very realistic problem of carbonation in concrete.[5]

Clearly, there are still many applications involving diffusion where CA could provide useful models and efficient numerical simulations. In particular, reaction-diffusion processes are responsible for several interesting phenomena of pattern formation[6-8] that are very difficult to analyze theoretically and numerically because they are described by a set of nonlinear partial differential equations. Another example is the problem of diffusion in inhomogeneous media, or the trapping problem where the randomly walking particles may disappear when reaching particular sites of the system. This kind of model can be applied to several physical situations[9] and has recently been investigated within a cellular automata approach.[10]

In view of such applications, it is important to have a reliable CA model of diffusion. It is not enough to have a rule which simulates qualitatively a diffusive behavior. One also needs a good quantitative agreement with real experiments. In particular, the artifacts of the model such as the discrete space and time should be irrelevant in the simulation.

CA approaches to diffusion have already been proposed by several authors. In ref. 11 a deterministic system of particles interacting via some particular collision rules is discussed. Assuming molecular chaos, one-dimensional diffusion is found to emerge from the rule. Unfortunately, numerical simulations of the model invalidate this hypothesis of molecular chaos and the macroscopic behavior does not follow the predicted diffusion equation.

Another approach that has been considered in the literature[12,2,4,5] consists of using a random CA. The idea is to produce synchronous random walks on a lattice, taking into account the exclusion principle (no more than one particle per site) often imposed on CA models. Although a qualitative diffusive behavior is observed, it is not clear in which limit these models really obey Fick's law of diffusion

$$\partial_t \rho = D\nabla^2 \rho \tag{1.1}$$

It turns out that a more careful analysis shows that these kinds of CA algorithms indeed introduce corrections to (1.1) that may affect the expected diffusive behavior for nonequilibrium situations, or for short times and small systems.[5,13]

In this paper, we discuss a CA model of diffusion which is in the same spirit as the ones proposed in refs. 2, 4, and 12, but is more general. The discrete dynamics is solved analytically. The limit when the lattice spacing

and the time step go to zero is calculated and compared with the actual behavior of a finite automaton.

We show that for an appropriate choice of the parameters of the rule, our CA model gives a very good approximation to the stationary diffusion equation (1.1), even for small size systems. We also discuss the time-dependent regime for a system with periodic boundary conditions. We compare the time evolution of the Fourier components of the density as predicted by the cellular automata dynamics with both Fick's law and the telegraphist equation. It is found that the parameters entering the rule play an important role, in particular, for the isotropy of the dynamics.

In addition to providing indications on how to choose the appropriate length and time scales in a numerical simulations, our results are interesting from a theoretical point of view: an important task of CA modeling is to derivee the macroscopic behavior of a system starting from its microscopic dynamics (the CA rule). The usual way is to assume molecular chaos, to replace the finite-difference equations by a truncated Taylor expansion, and to solved the so-obtained Boltzmann equation by an iterative method (typically, the Chapman–Enskog method). In general, none of the above steps are rigorous or well controlled. On the other hand, in our model, the link between the microscopic and the macroscopic levels can be achieved explicitly because exact solutions of the discrete dynamics are found.

From a numerical point of view, our algorithm is appropriate for an implementation on a massively parallel computer. On special-purpose machines such as CAM-6 or CAM-8[14] simulations of particles diffusing on a lattice can be run at a speed that cannot be attained with other computers.

This paper is organized as follows. In Section 2, the model is defined for a two-dimensional square lattice. For the sake of clarity, the macroscopic behavior of the automaton is first derived by a Taylor expansion of the discrete dynamics, up to second order in space and time. The continuity equation is obtained. As a consequence of the discreteness of the lattice, it is found that the particle current is not related to the velocity field and the density by the usual relation $\mathbf{J} = \rho \mathbf{u}$. The differential equation governing the CA dynamics differs from Fick's law by two terms: a contribution due to the momentum tensor and a second-order time derivative of the density. This second correction accounts for a finite speed of information propagation[15] and leads to a telegraphist-like equation.[16] The Green–Kubo relation for the diffusion constant and the extension of the rule to a three-dimensional space are briefly discussed at the end of Section 2.

Section 3 is devoted to a more complete analysis of the discrete Boltzmann equation and the results are then used in Section 4 in order to

find explicit solutions for some specific boundary conditions. Comparison of the CA dynamics with Fick's law and the telegraphist equation are considered.

In Section 5, we compare the performances of this algorithm with another one recently proposed. Finally, conclusions are drawn in Section 6.

2. THE MODEL

2.1. The CA Rule

Our model consists of particles moving along the main directions of a hypercubic lattice (a square lattice in 2D or a cubic lattice in 3D). At each time step, the directions of the lattice are rotated by an angle α_i chosen at random, with probability p_i, independently for each site of the lattice. The effect of this mechanism is to produce a synchronous random walk.

In order to be more specific, we shall now define our CA rule for the two-dimensional case. This corresponds to the situation studied numerically on a special purpose computer, the CAM-6.[12] The one- and three-dimensional extensions will be briefly discussed at the end of this section.

We consider a square lattice with particles moving horizontally and vertically. In one time step τ, they travel a distance λ, which is the lattice spacing. The random motion is then achieved by introducing random deviations in the trajectories of the particles. For reasons of implementation on a special-purpose computer, it is convenient to restrict the dynamics to a maximum of one particle per direction at each site (exclusion principle). To ensure this constraint during the evolution, the deviations are produced by rotating all the particles entering a site by the same angle. For a square lattice, the possible rotations are 0, $\pi/2$, π, and $3\pi/2$. For instance, if the site $\mathbf{r}$ is rotated by an angle $\pi/2$, a particle entering that site from the left will come out upward and, at the next time step, will enter the site north of $\mathbf{r}$. These rotations are performed independently for each site, with probabilities p_0, p_1, p_2, and p_3, respectively (see Fig. 1).

In this model, we choose to make these rotations uniform and data-blind, i.e., they are produced by an external mechanism which is the same for all sites and which is not affected by the number of particles entering the sites. This mechanism is not suitable for simulating nonlinear or inhomogeneous diffusion (D function of the density or of the position). However, if the p_i vary slowly enough so that their spatial derivative can be neglected, inhomogeneous situations can also be considered.

We introduce the occupation numbers $n_i(\mathbf{r})$ defined as the number of particles entering the site $\mathbf{r}$ at time t with a velocity pointing in direction

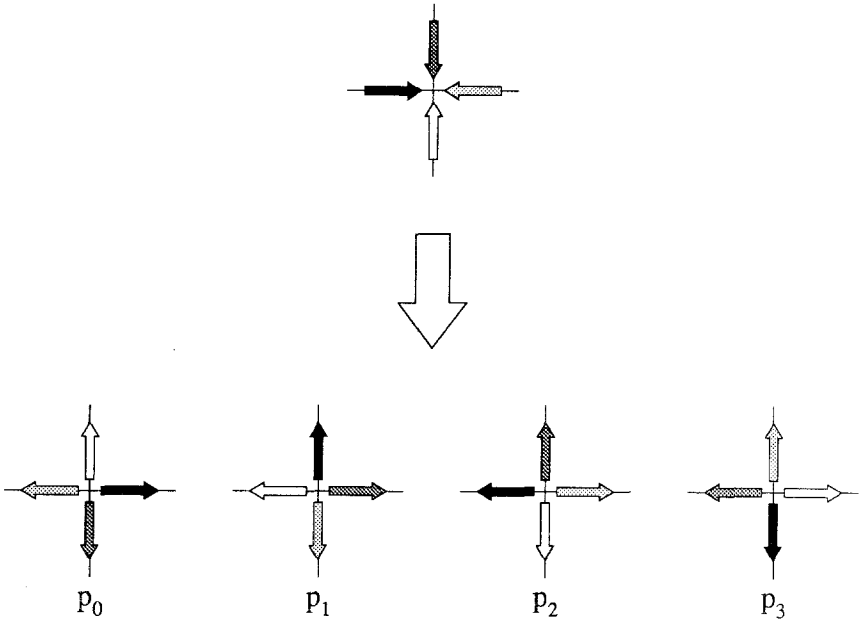

Fig. 1. How the entering particles are deflected at a typical site as a result of the rule. The four possible outcomes occur with respective probabilities p_0, p_1, p_2, and p_3. The figure shows four particles, but clearly, any one of the arrows can be removed when fewer entering particles are present.

$\mathbf{c}_i$ (see Fig. 2). As a consequence of the exclusion principle, n_i can be either zero or one.

The CA rule governing the dynamics of our model reads

$$n_i(\mathbf{r}+\mathbf{c}_i, t+\tau) = q_0 n_i(\mathbf{r}, t) + q_1 n_{i+1}(\mathbf{r}, t) + q_2 n_{i+2}(\mathbf{r}, t) + q_3 n_{i+3}(\mathbf{r}, t) \quad (2.1)$$

where i is defined modulo 4. The q_i are Boolean variables that are also

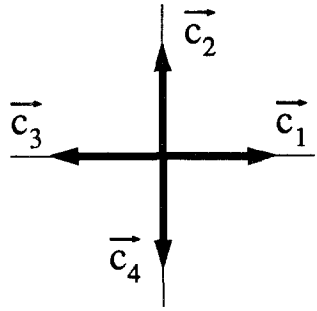

Fig. 2. The four directions of the lattice.

function of $\mathbf{r}$ and t, and which select only one of the four terms of the right-hand side of (2.1). More precisely, we define

$$(q_0; q_1; q_2; q_3) = \begin{cases} (1;0;0;0) & \text{with probability } p_0 \\ (0;1;0;0) & \text{with probability } p_1 \\ (0;0;1;0) & \text{with probability } p_2 \\ (0;0;0;1) & \text{with probability } p_3 \end{cases}$$

where

$$p_0 + p_1 + p_2 + p_3 = 1 \tag{2.2}$$

In practice (i.e., in the implementation on a dedicated CA computer such as CAM-6), the values of q_i can be produced in the following way: on the same lattice one runs another systems of particles that evolve according to some appropriate deterministic collision rules. For instance, a HPP gas[17] would be appropriate on a square lattice. The reason the HPP gas can be used as a random generator is that an ergodic behavior is expected in such a model. Thus, each possible configuration of the gas at a given site is supposed to appear with a probability depending only on the total number of particles. As explained in more detail in ref. 2, this fact can be used to select one of the above rotations necessary to produce the random walk. However, numerical experiments have shown that this mechanism is not perfect: the short-time correlations slightly renormalize the diffusion coefficient D if one does not let the random generator gas evolve several time steps before using it. But, as long as one is not interested in producing a given value of D, this effect does not seem important.

Equation (2.1) can be averaged over all possible realizations of the system. By defining $N_i(\mathbf{r}, t) = \langle n_i(\mathbf{r}, t) \rangle$, and remembering that the random generator is independent of the occupation numbers n_i, we obtain

$$N_i(\mathbf{r} + \mathbf{c}_i, t + \tau) = p_0 N_i(\mathbf{r}, t) + p_1 N_{i+1}(\mathbf{r}, t) + p_2 N_{i+2}(\mathbf{r}, t) + p_3 N_{i+3}(\mathbf{r}, t) \tag{2.3}$$

Equation (2.3) can be considered as the discrete Boltzmann equation associated with our system. It describes the evolution of the averaged occupation numbers N_i which range in the interval $[0; 1]$. This equation has two important features that are usually not present in most many-particles systems: our Boltzmann equation is exact (no truncation of a hierarchy is necessary) and linear. This makes the analytical study of our system quite interesting because the hard to control molecular chaos

hypothesis is true by construction of the dynamics. Linear Boltzmann equations are important in physics because explicit solutions can be obtained and compared with the approximation schemes generally used. An equation very similar to ours has been considered by Hauge.[18] The main difference is that in our case, space and time are discrete, which adds new features to the dynamics. Also, when the p_i are not all equal to 1/4, the solution proposed in ref. 18 cannot be adapted to our Boltzmann equation.

For isotropy reason, it is now natural to assume that the probability for a particle to be deflected by 90 deg left or right is the same. Thus, henceforth, we shall impose

$$p_1 = p_3 \equiv p \tag{2.4}$$

which implies

$$p_0 + 2p + p_2 = 1 \tag{2.5}$$

2.2. The Balance and the Telegraphist's Equations

We shall now derive the differential equation governing the evolution of the macroscopic quantity ρ, which is the density of particles. In this section, we are mainly interested in a simple derivation of the physical properties of our model. Thus, we shall assume that the Boltzmann equation (2.3) is still correct in the continuous limit, provided we replace the finite differences by a truncated Taylor expansion. This expansion will be considered up to second order in λ and τ. The validity of such a procedure will be studied in the next sections.

According to the usual relations of statistical mechanics, we define

$$\rho(\mathbf{r}, t) = \sum_{i=1}^{4} N_i(\mathbf{r}, t) \tag{2.6}$$

The velocity field $\mathbf{u}(\mathbf{r}, t)$ is then

$$\rho(\mathbf{r}, t)\, \mathbf{u}(\mathbf{r}, t) = \sum_{i=1}^{4} N_i(\mathbf{r}, t)\, \mathbf{v}_i \tag{2.7}$$

where

$$\mathbf{v}_i \equiv \frac{\lambda}{\tau} \mathbf{c}_i \tag{2.8}$$

We also introduce the momentum tensor $\Pi_{\mu\nu}$, which is defined using the Dirac notation

$$\Pi \equiv \sum_{i=1}^{4} N_i\, |\mathbf{v}_i\rangle\langle\mathbf{v}_i| \tag{2.9}$$

Our dynamics has the property of conserving the number of particles. Therefore, one expects a continuity equation to hold in our problem. Summed over i, Eq. (2.3) can be written as

$$\rho(\mathbf{r}, t) - \rho(\mathbf{r}, t-\tau) + \frac{\tau}{\lambda} \sum_{i=1}^{4} J_i(\mathbf{r}, t) = 0 \tag{2.10}$$

where $(\tau/\lambda) J_i$ is the net number of particles that have traveled between time $t-\tau$ and time t on the lattice link connecting $\mathbf{r}+\lambda\mathbf{c}_i$. In agreement with the interpretation of the N_i, it reads

$$J_i(\mathbf{r}, t) = \frac{\lambda}{\tau} [N_i(\mathbf{r}+\lambda\mathbf{c}_i, t) - N_{i+2}(\mathbf{r}, t)] \tag{2.11}$$

The factor of λ/τ has been added to give J_i the same units as $\rho\mathbf{u}$. Equation (2.10) has the form of a discrete continuity equation: when summed over the $\mathbf{r}$ in a rectangular patch of sites, all the $J_i(\mathbf{r})$ cancel except for the ones at the boundaries. It means that the variation of the number of particles in the considered region is given by the sum on its boundary of the quantity $(\tau/\lambda) J_i$, where i is such that $\mathbf{c}_i$ points outside the region.

It is important to notice that J_i is not equal to $\mathbf{c}_i \cdot \rho\mathbf{u}$, as is the case in a continuous space. Indeed, from (2.11) we have

$$\begin{aligned} J_i &= \frac{\lambda}{\tau} [N_i(\mathbf{r}) - N_{i+2}(\mathbf{r})] + \frac{\lambda}{\tau} [N_i(\mathbf{r}+\lambda\mathbf{c}_i) - N_i(\mathbf{r})] \\ &= \mathbf{c}_i \cdot \rho\mathbf{u} + \frac{\lambda}{\tau} [N_i(\mathbf{r}+\lambda\mathbf{c}_i) - N_i(\mathbf{r})] \end{aligned} \tag{2.12}$$

This difference between the particle flux and the velocity field in lattice gases usually appears as a correction to the transport coefficient due to the discretness of space.[19]

In the continuous limit, a Taylor expansion of (2.11) gives

$$J_i = \mathbf{c}_i \cdot \left[\rho\mathbf{u} + \frac{\lambda^2}{\tau} \operatorname{grad} N_i + \frac{\lambda^3}{2\tau} \operatorname{grad}(\operatorname{div} \mathbf{c}_i N_i) + \mathcal{O}(\lambda^4) \right] \tag{2.13}$$

and Eq. (2.10) takes the usual form of a continuity equation

$$\rho(\mathbf{r}, t) - \rho(\mathbf{r}, t-\tau) + \tau \operatorname{div} \mathbf{J} = 0 \tag{2.14}$$

where $\mathbf{J}$ is

$$\mathbf{J}(\mathbf{r}, t) = \rho\mathbf{u}(\mathbf{r}, t) + \frac{\tau}{2} \nabla \Pi(\mathbf{r}, t) + \mathcal{O}(\lambda^3) \tag{2.15}$$

Equation (2.14) expresses particle number conservation. Momentum is not conserved in our model, unless $p_0 = 1$. The dissipation rate of momentum is obtained by writing (2.3) in the form of a balance equation for $\rho\mathbf{u}$. After multiplication by $\mathbf{v}_i$ and summation over i, Eq. (2.3) reads

$$\rho\mathbf{u}(\mathbf{r}, t+\tau) - \rho\mathbf{u}(\mathbf{r}, t) + \tau\nabla(\Pi(\mathbf{r}, t+\tau) + \mathcal{O}(\lambda^3)) = -(1 + p_2 - p_0)\,\rho\mathbf{u}(\mathbf{r}, t) \tag{2.16}$$

A nonvanishing right-hand side in Eq. (2.16) is the reason for the nonconservation of momentum.

Relations (2.14) and (2.16) are not sufficient to give an equation for the density. Another useful relation is obtained by rewriting (2.3) for $\mathbf{r} = \mathbf{r} - \lambda\mathbf{c}_i$ and summing over i. After a Taylor expansion up to second order in λ, one gets

$$\rho(\mathbf{r}, t+\tau) = \rho(\mathbf{r}, t) - \lambda \sum_{l=0}^{3} \sum_{i=1}^{4} (\mathbf{c}_{i-l}\cdot\nabla)(p_l N_i(\mathbf{r}, t)) + \frac{\lambda^2}{2} \sum_{l=0}^{3} \sum_{i=1}^{4} (\mathbf{c}_{i-l}\cdot\nabla)^2 (p_l N_i(\mathbf{r}, t)) + \mathcal{O}(\lambda^3) \tag{2.17}$$

Using that $\mathbf{c}_i = -\mathbf{c}_{i-2}$, $p_1 = p_3 = p$, and

$$(\mathbf{c}_i\cdot\nabla)^2 + (\mathbf{c}_{i+1}\cdot\nabla)^2 = \nabla^2 \tag{2.18}$$

Eq. (2.17) becomes

$$\rho(\mathbf{r}, t+\tau) - \rho(\mathbf{r}, t) = \lambda^2\nabla^2(pq) - \tau\,\mathrm{div}[(p_0 - p_2)\,\rho\mathbf{u}] + \frac{\tau^2}{2}\partial_\mu\partial_\nu[(p_0 + p_2 - 2p)\,\Pi_{\mu\nu}] \tag{2.19}$$

where the right-hand side is taken at position $\mathbf{r}$ and time t. Here, μ and ν label the space coordinates x and y. Summation over repeated space indices is assumed.

The term $\mathrm{div}\,\rho\mathbf{u}$ can be eliminated using Eqs. (2.14) and (2.15). After a Taylor expansion of the finite time differences, we obtain

$$\partial_t\rho + \frac{\tau}{2}\frac{1 - p_2 + p_0}{1 + p_2 - p_0}\partial_t^2\rho = \frac{\lambda^2}{\tau}\frac{p}{1 + p_2 - p_0}\nabla^2\rho + \tau^2\frac{p_0 - p}{1 + p_2 - p_0}\partial_\mu\partial_\nu\Pi_{\mu\nu} \tag{2.20}$$

Some comments are now in order. By choosing $p_0 = p$, we obtain a closed equation for ρ and the right-hand side of (2.20) has exactly the form expec-

ted for a diffusion equation. On the other hand, (2.20) is a second-order differential equation in time. This is not the case for Fick's law [Eq. (1.1)]. In fact, our equation rather looks like the telegraphist equation,[16] in agreement with the results first obtained by Taylor for a model of a random walk with inertia.[20]

When $p_0 \neq 0$, the term containing the momentum tensor can be expressed as a function of the density only using the "local equilibrium" ansatz

$$N_i = \frac{\rho}{4} + \frac{1}{2}\frac{\tau}{\lambda}\mathbf{c}_i \cdot \rho\mathbf{u} \tag{2.21}$$

The momentum tensor then reduces to the scalar pressure and

$$\partial_\mu \partial_\nu \Pi_{\mu\nu} = \frac{1}{2}\left(\frac{\lambda}{\tau}\right)^2 \nabla^2 \rho$$

Equation (2.20) then takes the form of a standard telegraphist equation

$$\partial_t \rho + \frac{D}{c^2}\partial_t^2 \rho = D\nabla^2 \rho \tag{2.22}$$

where the diffusion constant D is

$$D = \frac{\lambda^2}{\tau}\frac{p + p_0}{4(p + p_2)} = \frac{\lambda^2}{\tau}\frac{p + p_0}{4[1 - (p + p_0)]} \tag{2.23}$$

and the speed of sound c is

$$c = \frac{\lambda}{\tau}\frac{1}{\sqrt{2}} \tag{2.24}$$

Equation (2.22) describes the behavior of our model in some appropriate limit. In principle, one expects contributions of all spatial and temporal derivatives. The presence of a second-order time derivative is conceptually important because information cannot travel faster than the particles themselves. This property emerges in our model because its dynamics is based on a microscopic picture of diffusion and noncausal effects cannot arise with a CA rule. In this respect, the telegraphist equation is more realistic than Fick's law of diffusion, although, in practice, the difference only shows up for large values of D.

Relation (2.23) shows that the diffusion coefficient D is adjustable by choosing the p_i. This fact is important when modeling a system containing

two or more species evolving on the same lattice with their own value of D. This situation appears in reaction-diffusion processes, where the various reagents may diffuse unequally.

2.3. The Three-Dimensional Case

In a three-dimensional space, our CA model of diffusion can be easily extended if the "rotations" that take place at each node of the lattice are properly chosen. On a cubic lattice, we have six possible directions of motion which can be mixed in several different ways, in order to produce random walk. Among the set of all the possibilities, one of them gives equations very close to the two-dimensional case. For this reason, we shall not repeat the details of the calculation. We shall simply describe how to produce the random walk and write down the corresponding telegraphist equation.

Let us first label the three main directions of the lattice by $\mathbf{c}_1$, $\mathbf{c}_2$, and $\mathbf{c}_3$, with the property that $\mathbf{c}_3 = \mathbf{c}_1 \times \mathbf{c}_2$. The three other directions are defined according to the relation

$$\mathbf{c}_i = -\mathbf{c}_{i+3}, \qquad i \text{ modulo } 6 \tag{2.25}$$

Now, we consider six operations R_k, $k = 0,..., 5$, that occur with probability p_i. The result of the operation R_k is to deflect the particle entering in the direction $\mathbf{c}_i$ into the direction $\mathbf{c}_{i+k}$. The discrete Boltzmann equation then reads

$$N_i(\mathbf{r} + \mathbf{c}_i, t + \tau) = \sum_{k=0}^{5} p_k N_{i+k}(\mathbf{r}, t) \tag{2.26}$$

Isotropy requires that we choose

$$p_1 = p_2 = p_4 = p_5 = p \tag{2.27}$$

As before, a contribution from the momentum tensor appears in the equation for the density, unless one imposes

$$p_0 = p \tag{2.28}$$

Otherwise, using the local equilibrium approximation

$$N_i = \frac{\rho}{6} \tag{2.29}$$

Eq. (2.26) leads to a telegraphist's equation for the average density ρ, with an adjustable coefficient of diffusion D. With

$$p_0 + 4p + p_3 = 1 \tag{2.30}$$

we obtain

$$D = \frac{\lambda^2}{\tau} \frac{1 + p_0 - p_3}{6(1 - p_0 + p_3)} = \frac{\lambda^2}{\tau} \frac{p_0 + 2p}{6[1 - (p_0 + 2p)]} \tag{2.31}$$

and a speed of sound

$$c = \frac{\lambda}{\tau} \frac{1}{\sqrt{3}} \tag{2.32}$$

Finally, for completeness, we briefly mention the one-dimensional case, which turns out to be quite simple because the momentum tensor is always proportional to the density. On a one-dimensional lattice, there are only two possible rotations and the dynamics is the following: the particles are either deflected by 180 deg with probability p_1, or continue in straight line with probability $p_0 = 1 - p_1$. Following the same procedure as before, one shows that the speed of sound is $c = \lambda/\tau$ and the diffusion constant $D = (\lambda^2/\tau)[p_0/2(1 - p_0)]$, $0 < p_0 < 1$.

2.4. The Mean Square Displacement and the Green–Kubo Formula

In Section 2.2, we obtained the value of the diffusion coefficient D by considering the dynamics of a system of particles performing a synchronous random walk, with an exclusion principle. The same coefficient D [as found in (2.23)] can also be obtained by considering only one particle and calculating its mean square displacement

$$\sigma^2(t) = \langle x^2(t) + y^2(t) \rangle$$

where

$$(x(t), y(t)) = \tau \sum_{n=0}^{t-1} \mathbf{v}(n)$$

and $\mathbf{v}(n)$ is one of the four possible velocities $\mathbf{v}_i = (\lambda/\tau)\,\mathbf{c}_i$ that a given particle has after n time steps. Since the probability of having a particle at a given site obeys the telegraphist equation (2.22), it is easy to show the following indentity, provided the probability and its gradient vanish on the boundaries:

$$D = \frac{1}{2d} \lim_{t \to \infty} \frac{\sigma^2(t)}{t} \tag{2.33}$$

where d is the dimension of the space. The expression for σ^2 can be easily calculated in our model. According to the CA rule, each particle performs a random walk, with probability p_0 of going straight, p_2 of bouncing back, and p of being deflected by 90 deg right or left. Thus, it is found that the mean square displacement is

$$\sigma^2(t) = t + 2(t-1)\frac{p_0 - p_2}{1 + p_2 - p_0} + 2\left(\frac{p_0 - p_2}{1 + p_2 - p_0}\right)^2 \times [(p_0 - p_2)^{t-1} - 1] \tag{2.34}$$

provided the lattice is infinite or the time short enough so that the particle has not reached the limit of the system. This relation leads to a value of D in perfect agreement with Eq. (2.23).

It is well known[18] that Eq. (2.33) is equivalent to a Green–Kubo relation. In our case, however, a correction due to the discreteness of the lattice is present.[21] After some algebra, (2.33) reads

$$D = \frac{\tau}{2}\sum_{n=0}^{\infty} \langle \mathbf{v}(0)\cdot\mathbf{v}(n)\rangle - \frac{\tau}{4}\langle \mathbf{v}(0)\cdot\mathbf{v}(0)\rangle \tag{2.35}$$

The last term in (2.35) has the same origin as the difference between the particle flux $\mathbf{J}$ and $\rho\mathbf{u}$ which we mentioned in Section 2.2.

Equation (2.33) provides a possible way of measuring the diffusion coefficient in a numerical simulation of our CA rule. When using a computer such as CAM-6, the statistics can be made very good by measuring $\langle y^2(t)\rangle$ for many particles starting all on the line $y=0$ and moving simultaneously. The value of D so obtained can be compared with the theoretical relation (2.23), thus providing a test of the random generator used for the simulation. For instance, when an HPP gas is used as a random generator, it is found that Eq. (2.33) is well satisfied, as long as the HPP dynamics is kept several times faster than the dynamics of the random walk (for instance, one reads the probabilities only once in every ten steps). Otherwise, we have observed some deviations between Eq. (2.23) and the measurement of D using relation (2.33).

3. THE DISCRETE DYNAMICS

Our aim is now to find an explicit solution of the discrete Boltzmann equation (2.3) for any value of the p_i, and to compare it with the solution of the continuous diffusion equation. Exact solutions of the discrete dynamics are of great interest because they allow us to obtain rigorously the macroscopic behavior of the automaton without having recourse to the

usual expansions (multiscale or Chapman–Enskog) whose convergence is difficult to check. This gives an estimation of the size of the system required for the continuum limit to be a good approximation and determines the time and length scales that provide a fair modeling of a diffusion process.

3.1. The Discrete Boltzmann Equation

Equation (2.3) can be written in the following matrix form:

$$TN(\mathbf{r}, t+\tau) = \Lambda N(\mathbf{r}, t) \tag{3.1}$$

where N is the column vector composed of the N_i, Λ is the four-by-four matrix

$$\Lambda = \begin{pmatrix} p_0 & p & p_2 & p \\ p & p_0 & p & p_2 \\ p_2 & p & p_0 & p \\ p & p_2 & p & p_0 \end{pmatrix} \tag{3.2}$$

and T is the matrix operator

$$T = \begin{pmatrix} t_1 & 0 & 0 & 0 \\ 0 & t_2 & 0 & 0 \\ 0 & 0 & t_3 & 0 \\ 0 & 0 & 0 & t_4 \end{pmatrix} \tag{3.3}$$

The translation operator t_i acting on any function $f(\mathbf{r})$ is defined as

$$t_i f(\mathbf{r}) \equiv f(\mathbf{r} + \mathbf{c}_i)$$

Since $\mathbf{c}_i = -\mathbf{c}_{i+2}$, the inverse of T is simply $T_{ij}^{-1} = \delta_{ij} t_{i+2}$.

The matrix Λ can be diagonalized with the linear transformation

$$P = \frac{1}{2}\begin{pmatrix} 1 & 1 & 1 & -1 \\ 1 & 1 & -1 & 1 \\ 1 & -1 & -1 & -1 \\ 1 & -1 & 1 & 1 \end{pmatrix} \quad \text{and}$$

$$P^{-1} = \frac{1}{2}\begin{pmatrix} 1 & 1 & 1 & 1 \\ 1 & 1 & -1 & -1 \\ 1 & -1 & -1 & 1 \\ -1 & 1 & -1 & 1 \end{pmatrix} \tag{3.4}$$

One finds

$$P^{-1}AP=\begin{pmatrix}1 & 0 & 0 & 0\\ 0 & p_0-p_2 & 0 & 0\\ 0 & 0 & p_0-p_2 & 0\\ 0 & 0 & 0 & 1-4p\end{pmatrix} \tag{3.5}$$

In terms of the new quantities M_i related to N_i by

$$N=PM \qquad \text{and} \qquad M=P^{-1}N \tag{3.6}$$

Eq. (3.1) can be rewritten as

$$P^{-1}TPM(t)=\begin{pmatrix}M_1(t-\tau)\\ (p_0-p_2)\,M_2(t-\tau)\\ (p_0-p_2)\,M_3(t-\tau)\\ (1-4p)\,M_4(t-\tau)\end{pmatrix} \tag{3.7}$$

Since all the M_i are taken at the same $\mathbf{r}$, the spatial dependence has been omitted in (3.7).

After some algebra, our problem reduces to two equations containing only M_1 and M_4,

$$\tau\hat{\partial}_t M_1+\frac{D_*}{c_*^2}\tau^2\hat{\partial}_t^2 M_1 = D_*(\delta_1+\delta_2+\delta_3+\delta_4)\,M_1+\frac{p_0-p}{4(p+p_2)}(-\delta_1+\delta_2-\delta_3+\delta_4)\,M_4 \tag{3.8}$$

$$a_4\tau\hat{\partial}_t M_4+b_4\tau^2\hat{\partial}_t^2 M_4+8p(p+p_2)\,M_4 = \frac{p_0+p}{2}(-\delta_1+\delta_2-\delta_3+\delta_4)\,M_1+\frac{p_0-p}{2}(\delta_1+\delta_2+\delta_3+\delta_4)\,M_4 \tag{3.9}$$

where $\hat{\partial}_t$ and $\hat{\partial}_t^2$ are the discrete time derivatives defined as

$$\hat{\partial}_t M_i\equiv\frac{1}{2\tau}[M_i(\mathbf{r},t+\tau)-M_i(\mathbf{r},t-\tau)] \tag{3.10}$$

$$\hat{\partial}_t^2 M_i\equiv\frac{1}{\tau^2}[M_i(\mathbf{r},t+\tau)-2M_i(\mathbf{r},t)+M_i(\mathbf{r},t-\tau)] \tag{3.11}$$

and the operator δ_i is given by

$$\delta_i=t_i-1 \tag{3.12}$$

The dimensionless diffusion constant D_* and speed of sound c_* are defined in agreement with Section 2 and read

$$D_* = \frac{p_0 + p}{4[1-(p+p_0)]} \qquad \text{and} \qquad c_*^2 = \frac{1}{2} \tag{3.13}$$

and the coefficients a_4 and b_4 are

$$a_4 = 1-(p_0-p_2)(1-4p) \quad \text{and} \quad b_4 = p + p_0 - 2p(p_0-p_2) \tag{3.14}$$

Similarly, it is found that M_2 and M_3 are related to M_1 and M_4 by

$$\begin{aligned} M_2 + a_2\tau\hat{\partial}_t M_2 + \frac{1}{2}\tau^2\hat{\partial}_t^2 M_2 \\ = -\frac{1}{2}\left(D_* + \frac{1}{4}\right)(\delta_1 + \delta_2 - \delta_3 - \delta_4) M_1 \\ + \frac{p_0 - p}{8(p_0+p)(p_2+p)}(\delta_1 - \delta_2 - \delta_3 + \delta_4) M_4 \end{aligned} \tag{3.15}$$

and

$$\begin{aligned} M_3 + a_3\tau\hat{\partial}_t M_3 + \frac{1}{2}\tau^2\hat{\partial}_t^2 M_3 \\ = -\frac{1}{2}\left(D_* + \frac{1}{4}\right)(\delta_1 - \delta_2 - \delta_3 + \delta_4) M_1 \\ + \frac{p_0 - p}{8(p_0+p)(p_2+p)}(\delta_1 + \delta_2 - \delta_3 - \delta_4) M_4 \end{aligned} \tag{3.16}$$

where

$$a_2 = a_3 = \frac{1+(p_0-p_2)^2}{4(p_0+p)(p_2+p)} \tag{3.17}$$

The relation between M and the density ρ and the velocity field $\mathbf{u}$ is easily obtained from the definitions (2.6) and (2.7). Equation (3.6) gives

$$\begin{aligned} \rho &= 2M_1 \\ \mathbf{c}_1 \cdot \rho\mathbf{u} &= \frac{\lambda}{\tau}(M_2 + M_3) \\ \mathbf{c}_2 \cdot \rho\mathbf{u} &= \frac{\lambda}{\tau}(M_2 - M_3) \\ 2M_4 &= -N_1 - N_3 + N_2 + N_4 \end{aligned} \tag{3.18}$$

It should be noted that for $p_0 = p$, we obtain a closed equation for $\rho = 2M_1$. Equation (3.8) simply reads

$$\hat{\partial}_t \rho + \frac{D}{c^2} \hat{\partial}_t^2 \rho = \hat{D} \hat{\nabla}^2 \rho \tag{3.19}$$

where $\hat{\nabla}^2$ is the discrete Laplacian operator defined as

$$\hat{\nabla}^2 \equiv \frac{1}{\lambda^2} (\delta_1 + \delta_2 + \delta_3 + \delta_4) \tag{3.20}$$

which tends to the true Laplacian ∇^2 in the limit $\lambda \to 0$. Relation (3.19) is a discrete form of the telegraphist equation. Similarly, when $p_0 = p$, the other M_i are only coupled to M_1.

3.2. The Stationary State

For a stationary state ($\hat{\partial}_t = \hat{\partial}_t^2 = 0$), it also possible to find a closed equation for $\rho = 2M_1$ by substituting M_4 from (3.9) into (3.8). By iterating this process, Eq. (3.8) can be rewritten as

$$\Delta_1 M_1 + \frac{\alpha}{\beta} \Delta_2 \left[\sum_{n=0}^{\infty} \left(\frac{\alpha}{\beta} \right)^n \Delta_1^n \right] \Delta_2 M_1 = 0 \tag{3.21}$$

where Δ_1 and Δ_2 are the following operators:

$$\Delta_1 \equiv (\delta_1 + \delta_2 + \delta_3 + \delta_4), \qquad \Delta_2 \equiv (-\delta_1 + \delta_2 - \delta_3 + \delta_4) \tag{3.22}$$

and

$$\alpha = \frac{p_0 - p}{p_0 + p} \qquad \text{and} \qquad \beta = \frac{16p(p + p_2)}{p + p_0} \tag{3.23}$$

Equation (3.21) allows us to consider the corrections to Laplace equation due to higher order space derivatives. With

$$\delta_1 + \delta_3 = \lambda^2 \partial_x^2 + \frac{2\lambda^4}{4!} \partial_x^4 + \mathcal{O}(\lambda^6)$$

and

$$\delta_2 + \delta_4 = \lambda^2 \partial_y^2 + \frac{2\lambda^4}{4!} \partial_y^4 + \mathcal{O}(\lambda^6)$$

Eq. (3.21) reads

$$\left[\lambda^2(\partial_x^2+\partial_y^2)+\lambda^4\left(\frac{2}{4!}+\frac{\alpha}{\beta}\right)(\partial_x^4+\partial_y^4)-2\lambda^4\frac{\alpha}{\beta}\partial_x^2\partial_y^2\right]M_1+\mathcal{O}(\lambda^6)=0 \quad (3.24)$$

Thus, to order $(\lambda/L)^2$, the density obeys the Laplace equation.

When $p_0=p$, or when M_4 can be neglected in comparison to M_1 (which is the case in first approximation), it is easy to calculate $\rho\mathbf{u}$ in a stationary state. Equations (3.15) and (3.16) give

$$M_2=-\frac{1}{2}\left(D_*+\frac{1}{4}\right)(\delta_1+\delta_2-\delta_3-\delta_4)\,M_1 \quad (3.25)$$

$$M_3=-\frac{1}{2}\left(D_*+\frac{1}{4}\right)(\delta_1-\delta_2-\delta_3+\delta_4)\,M_1 \quad (3.26)$$

and, with (3.18), we have

$$\rho\mathbf{u}=-\left(D_*+\frac{1}{4}\right)\frac{\lambda}{\tau}\left[\mathbf{c}_1\frac{1}{2}(\delta_1-\delta_3)+\mathbf{c}_2\frac{1}{2}(\delta_2-\delta_4)\right]\rho$$

Up to first order in λ, a Taylor expansion of the above equation leads to the relation

$$\rho\mathbf{u}=-\left(D+\frac{\lambda^2}{4\tau}\right)\text{grad}\,\rho \quad (3.27)$$

Thus, we do not have the usual relation $\rho\mathbf{u}=-D\,\text{grad}\,\rho$. As explained in Section 2, the reason is that here the particle current $\mathbf{J}$ is not equal to $\rho\mathbf{u}$, due to the discreteness of the lattice.

4. SOME EXACT RESULTS OF THE DISCRETE BOLTZMANN EQUATION

In this section we are going to solve our discrete equations (3.8) and (3.9) for a few boundary conditions and address the question of how the continuous limit converges toward the solution of the diffusion equation or the telegraphist equation. We shall see that the choice of the p_i is of importance and that significant deviations may appear in finite systems.

4.1. Density Profile for Diffusion between Parallel Source and Sink

Here we consider a system whose boundary conditions consist of two parallel lines of sites having a different evolution rule: the first line (the

source) is such that all the sites continually produce a particle in each direction, while on the other line (the sink), all entering particles are absorbed. Furthermore, we also assume that the sink and the source are parallel to the lattice direction $\mathbf{c}_1$ and that the system is infinite or periodic in that direction. Finally, we take the x axis collinear with the $\mathbf{c}_1$ direction and choose the y coordinates of the sink and the source to be, respectively, $y=-\lambda$ and $y=L+\lambda$. Therefore, our boundary conditions imply

$$N_2(y=0)=0 \qquad \text{and} \qquad N_4(y=L)=1 \tag{4.1}$$

These relations reflect the fact that no particle is entering the system near the source, whereas the source continually injects particles into it. By symmetry, the N_i vary only along the direction $\mathbf{c}_2$ and consequently,

$$\delta_1=\delta_3=0 \tag{4.2}$$

Let us now focus our attention on a stationary situation. With (4.2) and $\hat{\partial}_t=\hat{\partial}_t^2=0$, Eqs. (3.8) and (3.9) together yield

$$M_4=0 \tag{4.3}$$

Then, (3.8) reduces to

$$(\delta_2+\delta_4)\,M_1=0 \tag{4.4}$$

whose solution is simply

$$M_1=ay+b \tag{4.5}$$

In turn, Eqs. (3.15) and (3.16) give

$$M_2=-M_3=-\frac{1}{2}\left(D_*+\frac{1}{4}\right)(\delta_2-\delta_4)\,M_1=-\left(D_*+\frac{1}{4}\right)a\lambda \tag{4.6}$$

From Eqs. (3.6) and (3.4), one has

$$N_2=\frac{1}{2}(M_1+2M_2) \qquad \text{and} \qquad N_4=\frac{1}{2}(M_1-2M_2) \tag{4.7}$$

and thus

$$a=\frac{2}{L+4\lambda(D_*+\frac{1}{4})} \qquad \text{and} \qquad b=2\lambda\left(D_*+\frac{1}{4}\right)a \tag{4.8}$$

The density $\rho = 2M_1$ is then

$$\rho = \frac{4y + 8\lambda(D_* + \frac{1}{4})}{L + 4\lambda(D_* + \frac{1}{4})} \tag{4.9}$$

and $(\rho \mathbf{u})_y = 2(\lambda/\tau)\, M_2$ reads

$$(\rho \mathbf{u})_y = -\frac{\lambda^2}{\tau}\left(D_* + \frac{1}{4}\right)\partial_y \rho \tag{4.10}$$

These results show that the stationary density profile is linear for any value of the p_i and also when λ is not small compare to L. In the continuous limit (i.e., for $\lambda \to 0$), (4.9) reduces to

$$\rho = \frac{4y}{L} \tag{4.11}$$

Equations (4.7) allow us to calculate the number of particles leaving the system after each time step. According to Eq. (2.11), this number is

$$N_2(y + \lambda) - N_4(y) = -D_* \lambda \partial_y \rho \tag{4.12}$$

This equation provides an efficient way to measure the diffusion coefficient in a numerical experiment by counting the average number of particles absorbed on the sink at each time step of the automaton.

The flux along the y axis is then

$$J_y = \frac{\lambda}{\tau}\left[N_2(y + \lambda) - N_4(y)\right] = -D\partial_y \rho \tag{4.13}$$

Thus, the usual relation between the flux and the gradient of the density holds. The diffusion coefficient $D = (\lambda^2/\tau)\, D_*$ contains no correction due to the lattice, as opposed to Eq. (4.10).

The linearity of the density profile has been checked with numerical simulations of the model on the special-purpose computer CAM-6. A perfect agreement is obtained.

In addition, the effect of the second-order time derivative $(D_*/c^2)\, \hat{\partial}_t^2$ in (3.8) clearly shows up for a time-dependent numerical simulation (i.e., before the steady state is reached). Indeed, for a large value of D_* the ballistic motion of the particles plays an important role. In Fig. 3, we check the nonstationary density profile versus the one predicted by the usual diffusion equation. When the value of D_* was set to $D_* = 0.74$ (i.e., $\sqrt{D_*} > c$), the numerical simulation shows the expected deviation due to the "telegraphist's term."

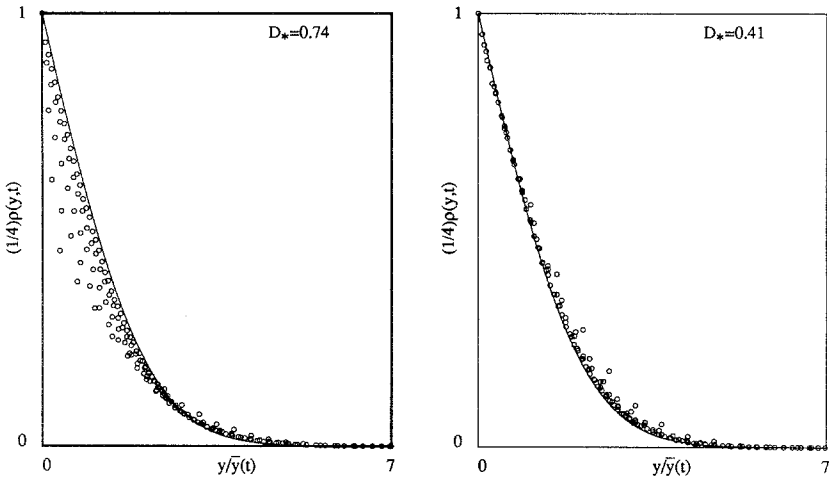

Fig. 3. Numerical simulations of the CA rule for a nonstationary situation. Particles emerge from a source at $y=0$. The system is periodic in the x direction and can be assumed infinite in the y direction. The plots show the results of measurements of $\rho(y, t)$ as a function of $y/\bar{y}(t)$, where $\bar{y}(t)$ is the center of mass of the diffusing particles. For a process obeying Fick's law, $\rho(y, t)=\operatorname{erfc}(y/\bar{y}(t))$, which is represented by the solid lines. The circles correspond to the measurements performed on the automaton with a value of $D_*=0.74$ in the left plot and $D_*=0.41$ in the right one. Significant deviations appear when D_* is large enough, as a result of the second-order time derivative in the telegraphist equation (ballistic motion).

4.2. The Semi-Infinite Strip

For more complex boundary conditions than the ones considered in the previous example, the stationary solution of (3.8) and (3.9) may be quite different from the solution of

$$\nabla^2\rho=0 \tag{4.14}$$

if the system is not large enough and the p_i not well chosen.

The geometry we are now going to consider has the shape of a well whose vertical walls are of infinite height and absorb particles, while the bottom line of the system acts as a source of particles. More precisely, we shall impose the following boundary conditions:

$$\rho(x=0,\ y)=\rho(x=L,\ y)=0, \qquad \text{for } y\geqslant 0 \tag{4.15}$$

$$\rho(x,\ y=0)=\phi=\text{cte} \qquad \text{for } 0<x<L \tag{4.16}$$

and

$$\lim_{y\to\infty}\ \rho=0 \tag{4.17}$$

The solution of (4.14) is known to be[22]

$$\rho = \frac{4\phi}{\pi} \sum_{n \text{ odd}} \frac{1}{n} \exp\left(-\frac{\pi y}{L}\right) \sin\left(\frac{\pi x}{L}\right) = \frac{2\phi}{\pi} \tan^{-1}\left(\frac{\sin(\pi x/L)}{\sinh(\pi y/L)}\right) \quad (4.18)$$

In order to solve (3.8) and (3.9) for the same boundary conditions, we first assume that $\mathbf{c}_1$ and $\mathbf{c}_2$ are respectively parallel to the x and y axes.

Next, we consider a solution of the following form for the M_i:

$$M_{1,4} = \sum_n A_{1,4}(n) \exp(z_n y) \sin(\omega_n x) \quad (4.19)$$

where

$$\omega_n = \pi n / L \quad (4.20)$$

and z_n has to be determined from (3.8) and (3.9), which, for a stationary state, can be rewritten as

$$(\delta_1 + \delta_2 + \delta_3 + \delta_4) M_1 + \alpha(-\delta_1 + \delta_2 - \delta_3 + \delta_4) M_4 = 0 \quad (4.21)$$

and

$$(-\delta_1 + \delta_2 - \delta_3 + \delta_4) M_1 + \alpha(\delta_1 + \delta_2 + \delta_3 + \delta_4) M_4 = \beta M_4 \quad (4.22)$$

where α and β are given by (3.23). Now, it should be noted that the functions $\exp(z_n y)$ and $\sin(\omega_n x)$ are eigenfunctions of the discrete operators $\delta_1 + \delta_3$ and $\delta_2 + \delta_4$:

$$(\delta_1 + \delta_3) \sin(\omega_n x) = b_\omega \sin(\omega_n x) \quad (4.23)$$

$$(\delta_2 + \delta_4) \exp(z_n y) = b_z \exp(z_n y) \quad (4.24)$$

and

$$(\delta_1 + \delta_3) \exp(z_n y) = (\delta_2 + \delta_4) \sin(\omega_n x) = 0 \quad (4.25)$$

where

$$b_\omega \equiv 2\left[\cos\left(\frac{\pi n}{L}\lambda\right) - 1\right] \quad (4.26)$$

and

$$b_z \equiv \exp(z_n \lambda) + \exp(-z_n \lambda) - 2 \quad (4.27)$$

After substitution of (4.19) into (4.21) and (4.22), we obtain

$$\begin{aligned}(b_\omega + b_z)\, A_1 + \alpha(-b_\omega + b_z)\, A_4 = 0 \\ (-b_\omega + b_z)\, A_1 + [\alpha(b_\omega + b_z) - \beta]\, A_4 = 0\end{aligned} \tag{4.28}$$

In order to have $A_{1,4} \neq 0$, we must choose b_z such that

$$b_z = \frac{b_\omega}{4(\alpha/\beta)\, b_\omega - 1} \tag{4.29}$$

Using (4.27), this result gives

$$\exp(z_n \lambda) = 1 + \frac{b_z}{2} \pm \frac{1}{2}(b_z^2 + 4b_z)^{1/2} \tag{4.30}$$

The important parameter of the problem is the ratio

$$\frac{\alpha}{\beta} = \frac{p_0 - p}{16p(p + p_2)} \tag{4.31}$$

Clearly, α/β can be made arbitrary large by choosing p small enough. On the other hand, its smallest value is

$$\frac{\alpha}{\beta} = -\frac{1}{8}$$

obtained for $p = 1/2$ and $p_0 = p_2 = 0$.

From (4.26), b_ω lies in the interval $[-4, 0]$. Thus, according to (4.29), b_z is always positive if $\alpha/\beta > -1/16$. On the other hand, for $-1/8 \leqslant \alpha/\beta \leqslant -1/16$, b_z is negative and less than -4 if $b_\omega < \beta/4\alpha$. Therefore, the square root in (4.30) is always real. In order to fulfill the boundary condition (4.17), one must have $|\exp(z_n \lambda)| < 1$. This is achieved by choosing the minus sign in front of the square root in (4.30) when $b_z \geqslant 0$, and the plus sign otherwise.

It is then straightforward to calculate the density $\rho = 2M_1$ from (4.19) because, for $y = 0$, our expansion is identical to (4.18). Therefore

$$\rho = \frac{4\phi}{\pi} \sum_{n \text{ odd}} \frac{1}{n} [\exp(z_n \lambda)]^{y/\lambda} \sin\left(\frac{\pi x}{L}\right) \tag{4.32}$$

Although the density is only defined on the lattice sites, Eq. (4.32) provides an interpolation of ρ between the sites. In addition, it is very appropriate for a comparison with the continuous situation. As an example, we have

calculated the density for a system of size $L = 29\lambda$, with $\phi = 4$. The solution (4.18) of the Laplace equation at $x = 13\lambda$ and $y = 12\lambda$ is

$$\rho = 1.3404065 \tag{4.33}$$

while Eq. (4.32) predicts $\rho = 1.3387$ if $\alpha/\beta = -1/8$, $\rho = 1.3412$ if $\alpha/\beta = 0$, $\rho = 1.4255$ if $\alpha/\beta = 4$, and $\rho = 1.7688$ if $\alpha/\beta = 23.5$.

The agreement with the solution (4.18) becomes better and better as the size of the system is increased. Since

$$\exp(z_n y) = \{[\exp(z_n \lambda)]^{L/\lambda}\}^{y/L}$$

the convergence of the discrete solution toward the continuous result can be checked by comparing

$$\exp(-\pi n) \qquad \text{with} \qquad [\exp(z_n \lambda)]^{L/\lambda}$$

This is shown in Fig. 4 for various values of λ/L and α/β. One sees that the significant deviations that occur if the system is small become rapidly

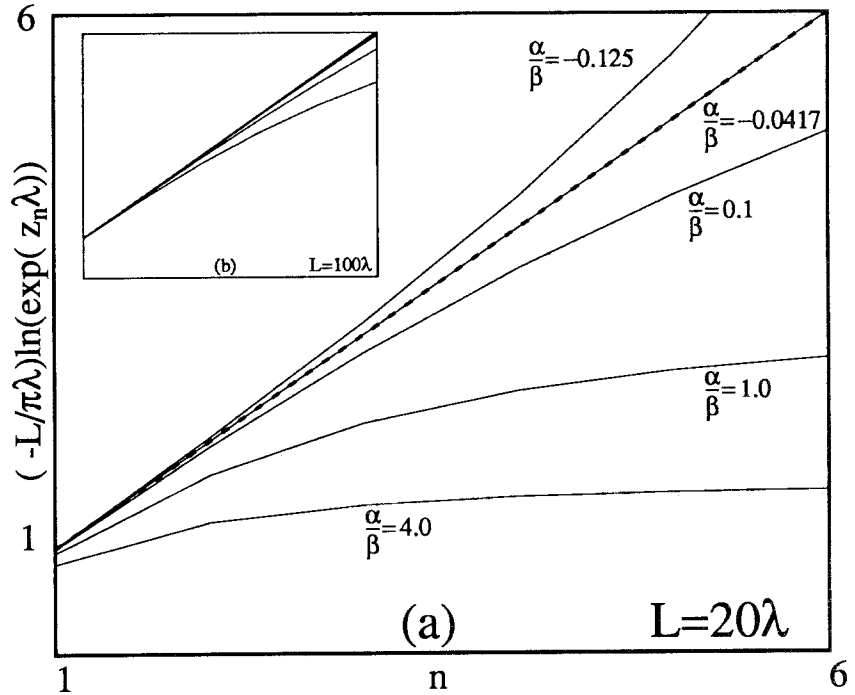

Fig. 4. Comparison between the solution of the Laplace equation and the solution of the CA dynamics for various values of α/β and for two system sizes (a) $L = 20\lambda$ and (b) $L = 100\lambda$. The dashed line corresponds to what should be obtained for a perfect agreement. This line turns out to coincide very well with $\alpha/\beta = -1/24 \approx -0.0417$.

negligible as the lattice spacing λ decreases. Figure 4 also suggests that there exists a value of α/β for which the solution of the discrete dynamics is very close to (4.18) (represented with the dashed line).

This value of α/β that gives the best approximation to the solution of Laplace equation can be obtained from Eq. (3.24). Assuming that $\nabla^2 M_1 \approx 0$, one has

$$2\partial_x^2 \partial_y^2 M_1 \approx -(\partial_x^4 + \partial_y^4) M_1$$

and, up to $\mathcal{O}(\lambda^6)$, (3.21) becomes

$$\lambda^2(\partial_x^2 + \partial_y^2) M_1 + 2\lambda^4 \left(\frac{1}{4!} + \frac{\alpha}{\beta}\right)(\partial_x^4 + \partial_y^4) M_1 = 0 \tag{4.34}$$

From this relation, it appears that the best choice is to take

$$\frac{\alpha}{\beta} = -\frac{1}{24} \approx -0.0417 \tag{4.35}$$

With this value of α/β, the solution of the discrete problem will approximate the continuous solution up to $\mathcal{O}((\lambda/L)^6)$.

Returning to our numerical example, Eq. (4.32) with $\alpha/\beta = -1/24$ gives

$$\rho = 1.3404065$$

which is indeed the correct result (4.33). This excellent agreement is also very clear from Fig. 4.

Thus, our discrete model may predict the solution of the Laplace equation very accurately, even for quite small systems. This fact is important in numerical simulations because one can obtain satisfactory results without using very large systems which require more computation resources.

Furthermore, it may be very realistic to have a small separation between the sinks of particles. When modeling a microscopically inhomogeneous system where particles are trapped or absorbed at randomly distributed sites, the impurities may be separated by only a few lattice spacings. The density ρ should depend as little as possible on the physically irrelevant parameters of the model, such as the discrete aspect of the space.

It is now interesting to return to the numerical simulations of our CA rule and measure the average density for a stationary situation corresponding to the one studied above. The experiment was conducted on the

CAM-6 machine for the particular size of the system $L = 29\lambda$. For the implementation we considered, the random generator was not perfect and we could not set the p_i very accurately. We first chose $\alpha \approx 0$ and $D_* \approx 1/4$ and the experiment gave $\rho = 1.3400$ with a time average made over 11,657 measurements. On the other hand, for $\alpha/\beta \approx 23.5$ (and $D_* \approx 0.74$), the measured density was $\rho = 1.255$ with a statistics of 13,547 events. This discrepancy with the expected result of 1.7688 (see above) is easily explained because the actual boundary conditions on the automaton did not correspond exactly to the theoretical solution (4.32). Indeed, as in Section 4.1, our boundary conditions consisted of a source and a sink of particles. This has the effect of controlling the number of particles entering the system near the boundary (i.e., the N_i), but it does not specify the density on the sites next to the source and the sinks, where (4.32) is valid. Although these boundary conditions are more realistic than those we used in the theoretical solution, they are less tractable analytically. However, for large enough systems or small values of D_*, both situations are equivalent.

This section has shown the importance of choosing properly the p_i. In Fig. 5, we sketch the possible values of the p_i and the resulting values of D and α/β.

4.3. The Time-Dependent System with Periodic Boundary Conditions

The functions M_i [given by (3.18)] can always be written as a discrete Fourier series

$$M_i(\mathbf{r}, t) = \sum_{\mathbf{k} \in V_k} A_i(\mathbf{k}, t) \exp(i\mathbf{k} \cdot \mathbf{r}) \tag{4.36}$$

where

$$A_i(\mathbf{k}, t) = \frac{1}{\mathcal{N}_1 \mathcal{N}_2} \sum_{\mathbf{r} \in V_r} M_i(\mathbf{r}, t) \exp(-i\mathbf{k} \cdot \mathbf{r}) \tag{4.37}$$

V_r denotes the set of all lattice points and the wave numbers $\mathbf{k} \in V_k$ are given by

$$\mathbf{k} = (k_1, k_2) = \frac{2\pi}{\lambda}\left(\frac{n_1}{\mathcal{N}_1}, \frac{n_2}{\mathcal{N}_2}\right) \tag{4.38}$$

with

$$n_j \in \left\{ -\frac{\mathcal{N}_j}{2}, \ldots, 0, 1, \ldots, \frac{\mathcal{N}_j}{2} - 1 \right\} \tag{4.39}$$

where $j = 1, 2$ and $\mathcal{N}_1$ and $\mathcal{N}_2$ are the numbers of sites along the directions $\mathbf{c}_1$ and $\mathbf{c}_2$ of the lattice (assumed to be even).

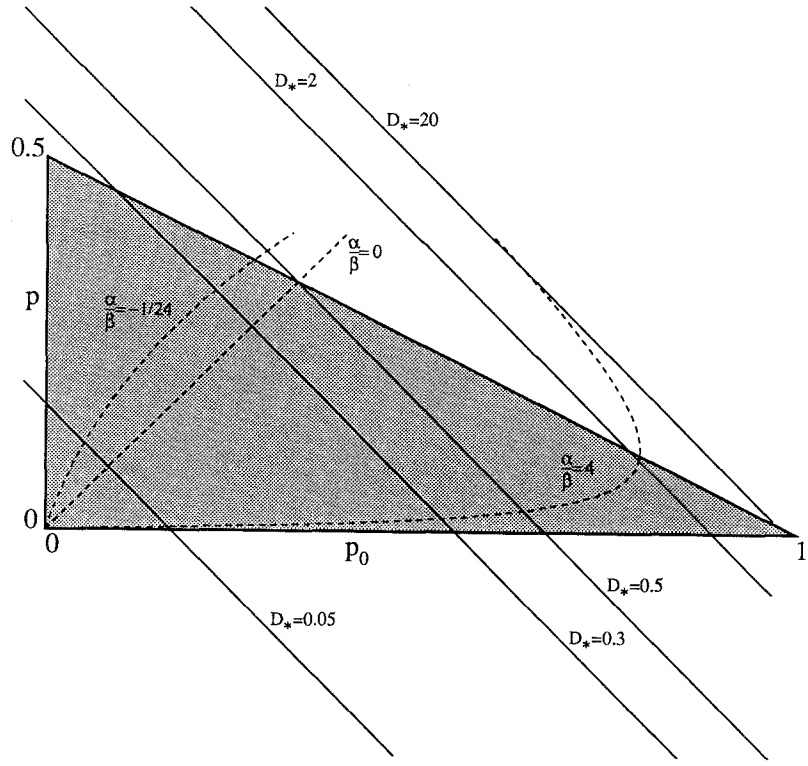

Fig. 5. Admissible values of p_0 and p and the curves $D_*(p_0, p) = D_*$ (solid line) and $(\alpha/\beta)(p_0, p) = \alpha/\beta$ (dashed line).

Simple equations of motion for the amplitude $A_i(\mathbf{k}, t)$ can be obtained when considering a system with periodic boundary conditions (wraparound lattice). In this case, no site has the status of being the boundary of the system and our equations for M_i [(3.8) and (3.9)] are valid for every $\mathbf{r} \in V_r$. Equations (3.8) and (3.9) lead to the following set of equations for the amplitudes $A_i(\mathbf{k}, t)$, uncoupled $\mathbf{k}$:

$$\begin{pmatrix} A_1(\mathbf{k}, t+\tau) \\ A_4(\mathbf{k}, t+\tau) \end{pmatrix} = B(\mathbf{k}) \begin{pmatrix} A_1(\mathbf{k}, t) \\ A_4(\mathbf{k}, t) \end{pmatrix} + C \begin{pmatrix} A_1(\mathbf{k}, t-\tau) \\ A_4(\mathbf{k}, t-\tau) \end{pmatrix} \tag{4.40}$$

where

$$B(\mathbf{k}) = \begin{pmatrix} (p_0+p)(\cos k_1\lambda + \cos k_2\lambda) & (p_0-p)(-\cos k_1\lambda + \cos k_2\lambda) \\ (p_0+p)(-\cos k_1\lambda + \cos k_2\lambda) & (p_0-p)(\cos k_1\lambda + \cos k_2\lambda) \end{pmatrix} \tag{4.41}$$

and

$$C=(p_2-p_0)\begin{pmatrix}1 & 0\\ 0 & 1-4p\end{pmatrix} \tag{4.42}$$

It is important to notice that this procedure no longer works when boundaries are imposed on the lattice because (3.8) and (3.9) are not true everywhere and cannot be summed over the entire lattice.

The solution of the iteration equation (4.40) is

$$\begin{pmatrix}A_1(\mathbf{k},t)\\ A_4(\mathbf{k},t)\end{pmatrix}=\sum_l e^{i\omega_l(\mathbf{k})t}\Phi_l(\mathbf{k}) \tag{4.43}$$

where ω_l and Φ_l are such that

$$\det(B(\mathbf{k})-e^{-i\omega_l\tau}C-e^{i\omega_l\tau}\mathbf{1})=0 \tag{4.44}$$

and

$$(B(\mathbf{k})-e^{-i\omega_l\tau}C-e^{i\omega_l\tau}\mathbf{1})\,\Phi_l=0 \tag{4.45}$$

Equation (4.44) is the dispersion relation of our model. With

$$\mu=e^{i\omega_l\tau} \tag{4.46}$$

it reads

$$(c_{11}\mu^{-1}-\mu+b_{11})(c_{22}\mu^{-1}-\mu+b_{22}\mu)-b_{12}b_{21}=0 \tag{4.47}$$

where b_{kl} and c_{kl} denote the elements of B and C. In general, we expect to find four solutions μ_l, associated with four vectors Φ_l, which is the number we need to specify A_1 and A_4 at times $t=0$ and $t=1$. Explicit solutions of (4.47) are difficult to find unless $c_{11}=c_{22}$ or $b_{12}=0$ ($b_{21}=0$ is not interesting since it corresponds to $p_2=1$).

The diffusive behavior of our dynamics causes all modes $\mathbf{k}\neq 0$ to vanish in the long-time limit. The long-lifetime modes are those for which μ is close to 1 in modulus. For $\mathbf{k}$ small enough, μ turns out to be real and the contour lines of the dispersion relation are easily obtained by writing (4.47) as

$$\cos k_2\lambda=\frac{\begin{array}{c}c_{11}c_{22}+\mu\cos k_1\lambda[c_{22}(p_0+p)+c_{11}(p_0-p)\\ -2p_0\mu^2]-\mu^2(c_{11}+c_{22}-\mu^2)\end{array}}{\begin{array}{c}\mu[c_{22}(p_0+p)+c_{11}(p_0-p)-2p_0\mu^2]\\ +4(p_0^2-p^2)\,\mu^2\cos k_1\lambda\end{array}} \tag{4.48}$$

This part of the dispersion relation corresponds to the dispersion relations of the diffusion and telegraphist equations, which read

$$\mu \equiv e^{i\omega\tau} = \exp[-D_*(\lambda k)^2] \tag{4.49}$$

and

$$\mu \equiv e^{i\omega\tau} = \exp\left\{-\frac{c_*^2}{2D_*}\left[1-\left(1-\frac{4D_*^2\lambda^2k^2}{c_*^2}\right)^{1/2}\right]\right\} \tag{4.50}$$

respectively. These three relations are compared in Figs. 6, by showing, for various values of D_*, their contour lines. It appears from these comparisons that a very good agreement is achieved for small wave vectors. When D_* increases, our discrete dynamics is closer to the telegraphist equation than to Fick's law.

The anisotropy of our model clearly shows up in Figs. 6, for large enough wave vectors. It is due to the terms $\cos k_1\lambda$ and $\cos k_2\lambda$ in (4.47) and is an effect of fourth order in $\mathbf{k}$. However, it is interesting to note that the isotropy can be much improved by properly choosing p, as illustrated in these plots. An isotropic dynamics is certainly an important constraint in a realistic model of diffusing particles. It is more important than an agreement with a particular diffusion equation (telegraphist or Fick's) which will never contain all the complexity of a real system.

As $\mathbf{k}$ increases, μ may have an imaginary part and we observe damped out waves. This phenomenon is also present in the telegraphist equation, but not in Fick's law. For instance, when $p_0 = p$ ($b_{12} = 0$ and $p \leqslant 1/3$), Eq. (4.47) yields

$$e^{i\omega\tau} = p[\cos k_1\lambda + \cos k_2\lambda] \pm \{(1-4p) + p^2[\cos k_1\lambda + \cos k_2\lambda]^2\}^{1/2} \tag{4.51}$$

For $1/4 < p \leqslant 1/3$ and

$$[\cos k_1\lambda + \cos k_2\lambda]^2 < \frac{4p-1}{p^2} \tag{4.52}$$

we write

$$e^{i\omega\tau} \equiv \mu e^{ic_*(\mathbf{k})k\lambda} \tag{4.53}$$

where μ is the modulus of $e^{i\omega\tau}$ and $c_*(\mathbf{k})$ is the (dimensionless) propagation speed of mode $\mathbf{k}$. We obtain

$$\mu = (4p-1)^{1/2} \tag{4.54}$$

and

$$c_*(\mathbf{k}) = \frac{1}{k\lambda}\operatorname{Arcos}\left(\frac{p}{(4p-1)^{1/2}}[\cos k_1\lambda + \cos k_2\lambda]\right) \tag{4.55}$$

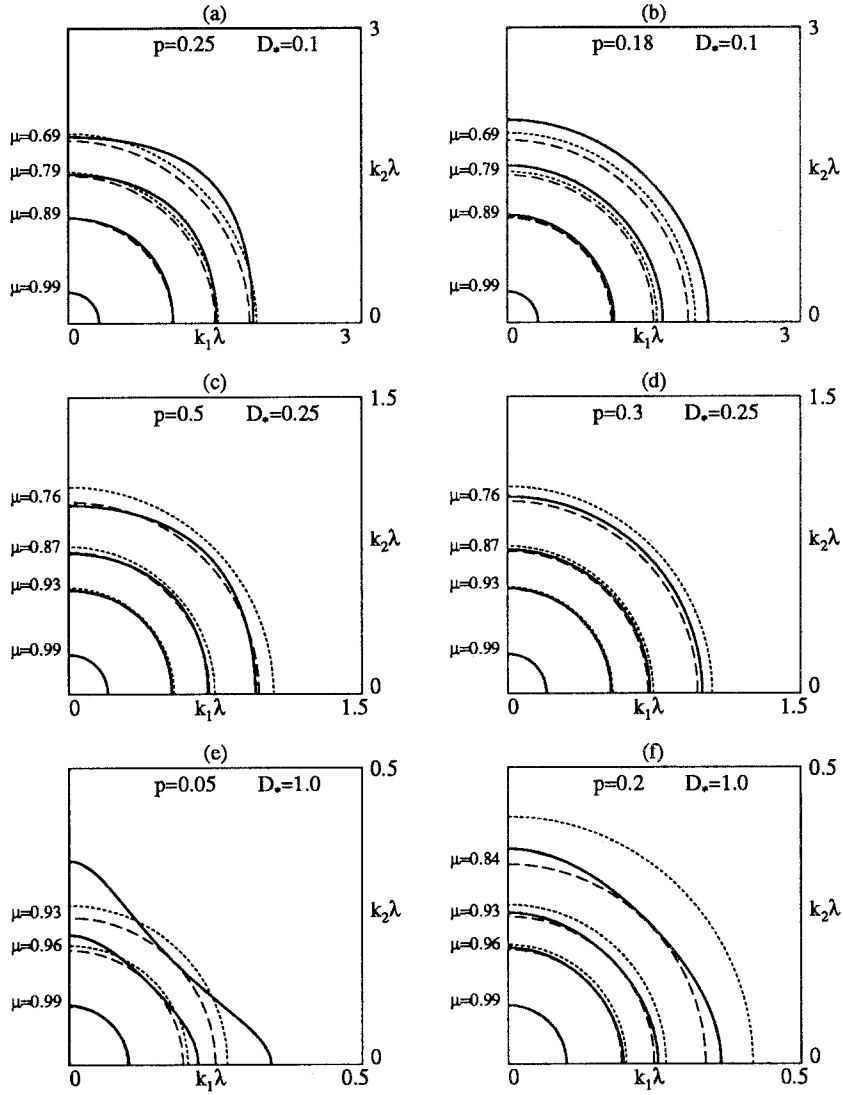

Fig. 6. Contour lines of the diffusive part of the dispersion relation $[\mu = \exp(i\omega\tau)]$ for various values of D_* and p. The solid lines correspond to the CA model, the dashed ones to the telegraphist equation, and the dotted ones to Fick's law of diffusion. For $\mu = 0.99$ the three dynamics are almost indistinguishable. Note that the scales are not the same in all figures.

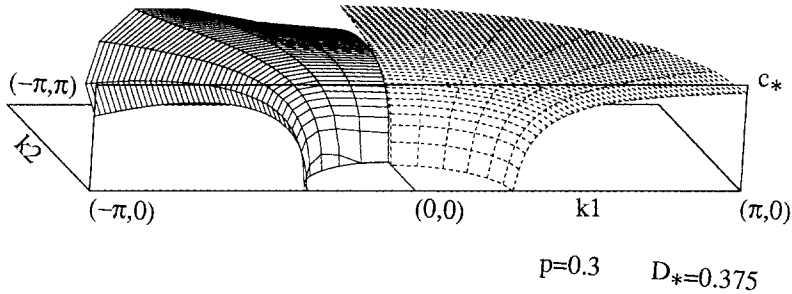

Fig. 7. Three-dimensional plot of the propagation speed of the mode **k**. The left surface (solid lines) represents $c_*(\mathbf{k})$ for the CA model and is invariant under $\pi/2$ rotations. The right part (dashed lines) corresponds to $c_*(\mathbf{k})$ given by the telegraphist equation and is invariant under any rotation.

Likewise, from (4.50), the propagation speed $c'_*(\mathbf{k})$ and the amplitude μ' predicted by the telegraphist equation are found to be

$$c'_*(\mathbf{k}) = \frac{c_*^2}{2D_* k\lambda}\left[\frac{4D_*^2(k\lambda)^2}{c_*^2} - 1\right]^{1/2} \tag{4.56}$$

and

$$\mu' = \exp\left(-\frac{c_*^2}{2D_*}\right) \tag{4.57}$$

These two speeds $c_*(\mathbf{k})$ and $c'_*(\mathbf{k})$ are compared in Fig. 7. Although they look qualitatively similar, they are quantitatively different. In particular, the anisotropy of the propagation speed is visible in the discrete model. However, these waves are not very significant for this value of D_* since they are quickly damped out due to the small value of μ.

5. COMPUTATIONAL ASPECTS

In this section we shall compare the performances, in terms of speed, of our cellular automata algorithm with another algorithm recently proposed in the literature.

One of the computational advantage of cellular automata algorithms is the fact that they can be implemented on special-purpose computers. Our algorithm has been implemented on such a machine, the CAM-6,[12] which is a very cheap board ($\sim$1500$) running in a PC. A system up to 128×128 has been simulated at a rate of 32 updatings of the entire system per second (i.e., 2×10^{-6} sec per site). For the improved version CAM-8, which shall

be completed soon (costing $\sim$10,000\$), systems much larger (typically 1024×1024) can be simulated and the time to update one site is reduced to 3×10^{-8} sec. Note that several CAM-6 or CAM-8 boards can be put together to consider larger systems without slowing down the simulation.

A naive implementation of the algorithm on a Connection Machine leads to a speed of about 7×10^{-7} sec per site, for a system size of 256×256.

The same algorithm running on a computer with no parallel architecture is slower. For example, on a VAX 8700, using multispin coding, the time to update one site is increased to 4×10^{-6} sec for a 256×256 lattice.

Pätzold *et al.*[23] have proposed a different algorithm for diffusion which is completely vectorizable on a Cray-like computer. This algorithm is based on Kawasaki exchange process at infinite temperature and has no obvious way to adjust the diffusion constant. Vectorization is possible by dividing the system into several sublattices. The time to update one site on a CRAY X-MP/416 computer is 5×10^{-7} sec.

Those figures show the efficiency of special-purpose computers, provided performance algorithms can be designed.

6. CONCLUSIONS

We have shown that a simple probabilistic CA algorithm was able to simulate very well the simultaneous random walk of many particles. The imposed exclusion principle as well as the correlated motion of the particles at a given site do not affect the expected diffusive behavior.

Macroscopically, the model obeys the telegraphist's equation, due to the finite speed of propagation of the particles. This introduces corrections to Fick's law only for large values of the diffusion constant and for short time, and gives the model a sensible physical content.

The parameters of the rule (the probabilities p_i) allow us to adjust the diffusion constant and are found to play an important role in the finite-size effects and the isotropy of the dynamics.

Implementation of the algorithm on a special-purpose computer such as CAM-8 leads to the fastest simulations of a system of diffusing particles. The fact that dedicated machines are much more affordable than a supercomputer is another reason to consider the CA approach to diffusion. Furthermore, by adding a reaction term in the CA rule, our model is appropriate to study many interesting and difficult reaction-diffusion problems. Such applications are now under investigation and have already given promising results.[24]

One of the great merits of the proposed model, as compared to previous cellular automata algorithms, is that a complete and exact theoretical

analysis of its properties can be performed. This fact is very interesting in two respects.

First, from the point of view of numerical simulations, our results provide us with some prescriptions on how to choose the suitable time and length scales in a given situation. The role played by the finite-size effects can be controlled as explained in Section 4. Pertinent information about the stationary states and the time evolution can be obtained.

Second, from the theoretical point of view, our model helps to develop a better understanding of many problems common in CA modeling of physical situations. In particular, it shows clearly how the multiscale aspect of the problem appears and the need to consider a different time scale for the propagative and dissipative regimes. Also, the effect of the lattice on the transport coefficients turns out to have a natural and simple interpretation. The fact that the associated Boltzmann equation is linear allows us to obtain exact solutions without uncontrolled approximations. Several important questions, such as the role played by the discreteness of space and time, the domain of validity of the continuous limit, and the convergence of the multiscale expansion[19] often used to solve discrete Boltzmann equations, can be answered. This last question will be the subject of a forthcoming publication.[25]

ACKNOWLEDGMENT

This work was supported by the Swiss National Science Foundation.

REFERENCES

1. G. Doolen, ed., *Lattice Gas Methods for Partial Differential Equations* (Addison-Wesley, 1990).
2. B. Chopard, M. Droz, and M. Kolb, *J. Phys. A* **22**:1609 (1989).
3. B. Chopard and M. Droz, *J. Phys. A* **21**:205 (1988).
4. D. Dab and J. P. Boon, in *Cellular Automata and Modeling of Complex Physical Systems*, P. Manneville, ed. (Springer-Verlag, 1989), p. 257.
5. E. Bonomi and L. M. Brieger, *J. Comp. Phys.* (1990).
6. R. E. Liesegang, *Naturwiss. Wochenschr.* **11**:353 (1896).
7. G. T. Dee, *J. Stat. Phys.* **39**:705 (1985).
8. L. Gálfi and Z. Rácz, *Phys. Rev. A* **38**:3151 (1988).
9. G. H. Weiss, *Am. Sci.* **71**:65 (1983).
10. A. Canning and M. Droz, *Physica D* **45**:285 (1990).
11. B. M. Boghosian and C. D. Levermore, in *Discrete Kinetic Theory, Lattice-Gas Dynamics and Foundation of Hydrodynamics*, R. Monaco, ed. (World Scientific, 1989).
12. T. Toffoli and N. Margolus, *Cellular Automata Machines: A New Environment for Modeling* (MIT press, Cambridge, 1987).
13. B. Chopard and M. Droz, in *Cellular Automata and Modeling of Complex Physical Systems*, P. Manneville, ed. (Springer-Verlag, 1989), p. 130.

14. N. Margolus and T. Toffoli, *Lattice Gas Methods for Partial Differential Equations*, G. Doolen, ed. (Addison-Wesley, 1990), p. 219.
15. T. Toffoli, unpublished; M. A. Smith, *Physica D* **660** (1990).
16. P. M. Morse and H. Feshbach, *Methods of Theoretical Physics* (McGraw-Hill, 1953), p. 865.
17. U. Frisch, D. d'Humières, B. Hasslacher, P. Lallemand, Y. Pomeau, and J.-P. Rivet, *Complex Systems* **1**:649 (1987). [Reprint in ref. 1.]
18. E. H. Hauge, in *Transport Phenomena*, G. Kirczenow and J. Marro, eds. (Springer, 1974), p. 337.
19. U. Frisch and J. P. Rivet, *C. R. Acad. Sci.* **303**(II):1065 (1986). [Reprint in ref. 1.]
20. G. I. Taylor, *Proc. Math. Soc.* **20**:196 (1921).
21. X. P. Kong and E. G. D. Cohen, *Phys. Rev. B* **40**:4838 (1989).
22. J. D. Jackson, *Classical Electrodynamics*, 2nd ed. (Wiley, 1975), p. 72.
23. O. Pätzold, submitted to *Comp. Phys.*
24. B. Chopard and M. Droz, *Euro. Phys. Lett.* (1991), to appear.
25. B. Chopard and M. Droz, in preparation.